Chapter 9
Nanostructured SnO_2 as CBRN Safety Material

V. Grinevych, V. Smyntyna, and L. Filevska

Abstract The present review briefly reflects tin dioxide applications for safety devices for the last 2 years as convenient, cheap, widespread material with suitable physical and chemical properties. The usage of nanoscale SnO_2 forms are considered for several types of devices such as: gas sensors of conductometric type, electrochemical sensors, sensors on the SPR effect, material for electrodes of lithium-ion batteries and solar cells, together with catalytic applications for decomposition of pollutants.

Keywords Tin dioxide · Gas sensing · Electrode material · Catalysts

9.1 Introduction

Tin dioxide, used for many years for various applications, is a well known material for researchers. It may seem that its properties have long been studied [1], the possibilities are exhausted and this material has any prospects. However, mastering the nanotechnologies has expanded the possible applications for many long-known materials, including tin dioxide. This position is supported due to tin dioxide active mentioning in the latest 10–12 years in a number of scientific reviews on gas sensors' [2–5], catalytic, and electrode materials [6, 7], as well as reviews on the manufacture, properties and application of various forms of this material [8–13]. There is also a work where nano tin dioxide is applied as sorbent in medical purposes [14].

This review of works (authors' inclusive) over the past 2 years supports the idea of nano tin dioxide as a cheap widely available material with convenient physicochemical properties for the devices of safety production.

V. Grinevych (✉) · V. Smyntyna · L. Filevska
Odessa I.I. Mechnikov National University, Odessa, Ukraine
e-mail: grinevich@onu.edu.ua

J. Bonča, S. Kruchinin (eds.), *Nanostructured Materials for the Detection of CBRN*,
NATO Science for Peace and Security Series A: Chemistry and Biology,
https://doi.org/10.1007/978-94-024-1304-5_9

Some tin dioxide applications (not complete) as a CBRN material are given below:

Sensors material: flammable and toxic gas sensors, heavy metal ion sensors, sensors of biologically dangerous objects.

Electrode end Catalytic applications: Li-ion batteries, solar cells, hydrogen and ozone production, the decomposition of pollutants.

Tin dioxide mentioning data in literature over the past year is given below (NCBI databases PubMed Central® (PMC) – free full-text archive of biomedical and life sciences journal literature in the U.S.; National Institute of Health, National Library of Medicine (NIH/NLM)): Total number of articles about tin dioxide is ~448, among them: nano SnO_2 – 231, sensors on SnO_2 – 186, SnO_2 electrode – 308, from them for solar cells – 118, for Li-Ion Battery – 63.

Over the past 10 years, more than a dozen scientific reviews on its properties, applications, research and developments with its use have been published.

9.2 Tin Dioxide in Sensor Applications

The spectrum of sensory materials for ensuring the safety of industrial, domestic, natural environments and the detection of toxic and dangerous components is currently estimated at tens. Among them, a whole class of metal oxides, which have been used for many years. One of the first places in this class belongs to tin dioxide. Its sensory properties, reduced to nanoscale, are much more effective.

The number of ways to register the environment compositions deviations from the standard has also increased. The conductometric methods used for more than 40 years were complemented by optical ones (control of direct absorption/reflection of light, a luminescence, use of methods of automatic calculation and comparison of optical characteristics of materials in the process of measurement), plasmon resonance and other methods. It was found that in the most of them the nano tin dioxide was very productive as a sensitive or matrix element.

9.2.1 Tin Dioxide as the Conductometric Type Adsorptive and Sensitive Element for Gas Sensors

An active study of tin dioxide gas sensitivity mechanisms to various polluting gases, as H_2, Cl_2, SO_2, and NH_3, NO, NO_2, CO, CO_2, CH_4, and C_3H_8, ethanol, acetone, etc., was applied for gas sensors production. The main role in sensitivity belongs to the active forms of oxygen (O_2^-, O^-, O^{2-}) adsorbed on the surface of the sensor material. The SnO_2, due to its chemical characteristics, adsorbs oxygen precisely in such active forms.

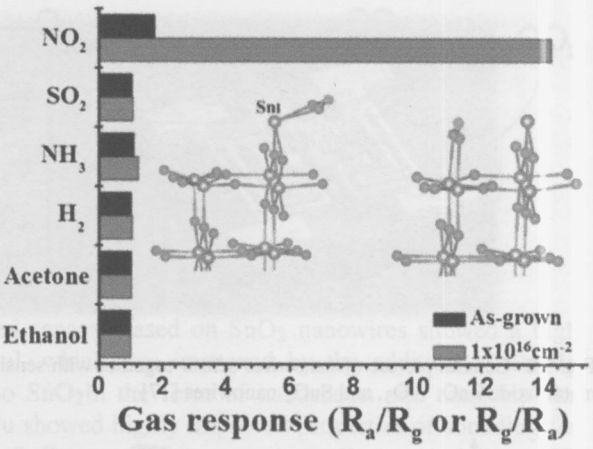

Fig. 9.1 Comparison of the sensitivity of nanowires of tin dioxide to various gases [15]. The inset shows the crystalline structure of SnO_2 nanowires

The work [15] is devoted to improvement of selectivity to NO_2 in SnO_2 nanowires by means of He ions radiation with different ion flux density. The maximum sensitivity to NO_2 shows the nanowire under ion flux density of 1×10^{16} ions/cm^2. The greatest number of surface defects in the form of interstitial tin was detected by photoluminescence analysis and X-ray photoelectron spectroscopy in the wires. Just these defects created by ionic radiation provide the adsorption of NO_2. The molecular modeling for the irradiated surface of SnO_2 (110) was carried out in the work. The Fig. 9.1 shows the comparison of sensitivity of tin dioxide nanowires to various gases and the crystalline structure of SnO_2 nanowires.

Theoretical studies of gas sensitivity mechanisms of SnO_2 (110) surface to mono and dioxide of nitrogen are conducted in work [16]. The phase diagram of the SnO_2 (110) surface in contact with O_2 and NO gas environment was determined by means of ab initio thermodynamic method. It was found that the fully reduced surface containing the bridging and in-plane oxygen vacancies was under oxygen-poor conditions, while the fully oxidized surface containing the bridging oxygen atoms and the oxygen dimer is under oxygen-rich conditions. The stoichiometric surface was proved to be the most stable. NO-rich conditions were formed by NO adsorption on the most stable surfaces only in the presence of oxygen.

Researchers from the Hanoi University of Science and technologies [17] made metal-oxide nanowires (NW) sensors for chlorine monitoring of ZnO, WO_3, and SnO_2 by on-chip growth technique with chemical vapor deposition method. The adsorptive response (R_{Cl2}/R_{air}) of SnO_2 nanowires sensor detecting 50 ppb Cl_2 at 50 °C was the largest and amounted about 57 units. Figure 9.2 shows general picture of nanowires sensor and sensitivity to chlorine comparison for metal-oxide nanowires of ZnO, WO_3, and SnO_2.

Tin dioxide was chosen by China researchers as a material for creation various three-dimensional nanostructures for sounding of gases [18]. By means of single-stage hydrothermal approach and the subsequent thermal annealing 3D nanostructures with various hierarchical morphology and, respectively, various

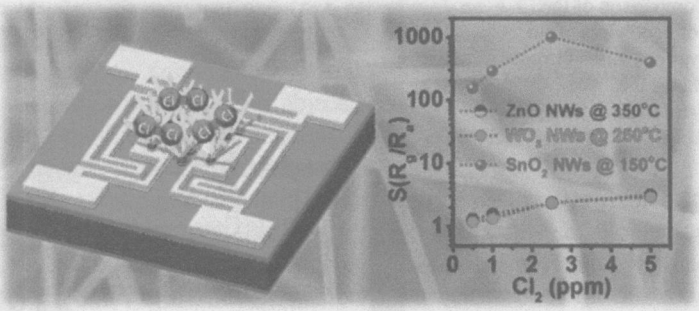

Fig. 9.2 General picture of nanowires sensor together with sensitivity comparison to chlorine of metal-oxide ZnO, WO_3, and SnO_2 nanowires [17]

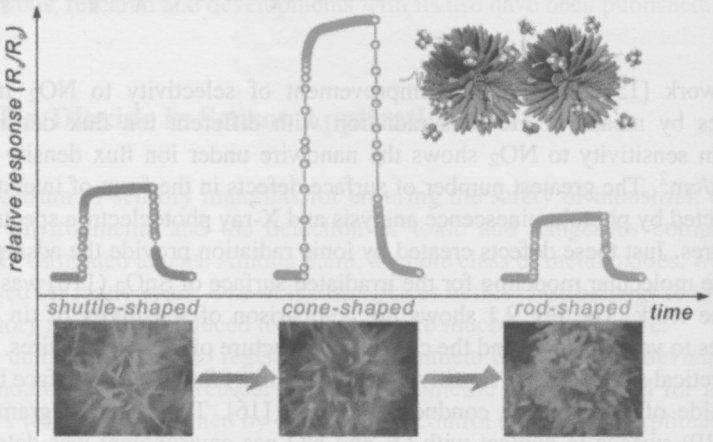

Fig. 9.3 A comparison of sensitivity to acetone of 3D nanostructures with various hierarchical morphology [18]

gas-sensitive properties were created. As it appeared the three-dimensional SnO_2 of cone-shaped hierarchy nanostructure shows the maximum sensitivity about 175 in relation to 100 ppm of acetone. A good sensitivity was shown by these structures also to some other organic compounds. As the microstructural analysis showed, the best sensitivity of cone-shaped hierarchical nanostructures is provided by more active superficial defects and discrepancies formed in the course of thermal recrystallization. A comparison of sensitivity to acetone of 3D nanostructures with various hierarchical morphology is shown at Fig. 9.3.

For improvement of sensor properties, increase in selectivity, the tin dioxide was doped by Cu [19, 20], Zn, Mn [21], Au [22], Sb and other additives. The study [19] of pure and copper-doped nanowires of tin dioxide, synthesized by thermal evaporation showed a good incorporation of copper atoms into the tetragonal rutile

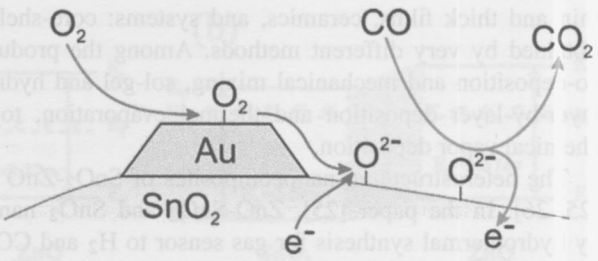

Fig. 9.4 Scheme of additional adsorption of oxygen on gold with its transfer to the surface of tin dioxide [22]

lattice of SnO_2. The undoped sensors based on SnO_2 nanowires showed a high sensitivity to gaseous ethanol, which was improved by the addition of Cu. In the other research [20], nano SnO_2in the form of nanosheets and nanodisc-like structures doped by 1% of Cu showed highly improved properties of sounding for CO in comparison with pure SnO_2 nanostructures and excellent selectivity to CO with insignificant hindrances by CH_4, CO_2 and NO_2. In the work [21] the SnO_2 doped by Cu (II) ions showed the fastest response time to 100 ppm of ethanol (9.7 sec. in comparison with 12.4 sec. for not doped SnO_2). At the same time, SnO_2 containing 2.91% of Mn showed 2.5 times higher response at detection of 100 ppm of ethanol in comparison with not doped material.

In [22] the sensitivity of tin dioxide covered with gold particles to gaseous CO was studied. The mechanism of sensitivity increasing was associated with additional adsorption of oxygen on gold with its transfer to the tin dioxide surface. Negatively charged oxygen ions on tin dioxide surface give additional states for interaction with the detected gas, thus increasing productivity of a sensitive layer. Figure 9.4 shows scheme of additional adsorption of oxygen on gold with its transfer to the surface of tin dioxide.

Tin dioxide is applied in the gas analysis not only as independent gas-sensitive material, but also as a constituent in composites, heterostructures and complex nanostructures for gas sounding. At the same time, its main role in a complex material is a gas-sensitive role, since it due to its structure changes its electrical parameters when interacting with the external environment [23]. Other materials provide selectivity by means of their catalytic features.

The work [24] is devoted to the research of such gas-sensitive nanoheterostructures as TiO_2/SnO_2 for H_2 control. The structures themselves were nanocrystalline TiO_2/SnO_2 n–n heterojunctions and have been obtained using flame spray synthesis from nanopowders of pure SnO_2, 90 mol % SnO_2/10 mol % TiO_2, 10 mol % SnO_2/90 mol % TiO_2 and pure TiO_2. It is interesting that with a long recovery time of SnO_2-rich samples their H_2 detection threshold is lower than 1 ppm and their large responses is over the whole measuring range. Researchers systematized the data on sensor response value, working temperature of gas-sensitive nanoheterostructures of TiO_2/SnO_2 and correlating with these data on structure and methods of material production. Such systemizing gave information on heterostructures in the form of nanopowders, nanofibres, nanotapes, nanowires,

thin and thick films, ceramics, and systems: core-shell, the coral-like structures obtained by very different methods. Among the production methods there are a co-deposition and mechanical mixing, sol-gel and hydrothermal methods, atomic layer-by-layer deposition and thermal evaporation, together with metal-organic chemical vapor deposition.

The heterostructured nanocomposites of SnO_2-ZnO were studied in the works [25, 26]. In the paper [25], ZnO-SnO_2 and SnO_2 nanoparticles were fabricated by hydrothermal synthesis for gas sensor to H_2 and CO. Heterostructures showed hypersensibility to the detected gases in comparison with undecorated SnO_2 nanoparticles. This result, together with the nano grain size, is explained by additional number of reaction states at the heterojunctions ZnO-SnO_2 nanoparticles where there can be noticable electron transfer between the compound nanostructures and the absorbed oxygen species.

Group of researchers [26] studied sensitive properties of SnO_2-ZnO composite nanostructured thin films series with different amounts of SnO_2 (from 0 to 50 wt %) for highly toxic and flammable gases (CO, CO_2, CH_4, and C_3H_8). Samples were deposited on a miniaturized porous alumina transducer using the sol-gel and dip coating method. Improved sensing was achieved for the ZnO (98 wt %) – SnO_2 (2 wt %) composite as compared to the sensors containing only the pristine oxides. Actually, only 2 wt % of tin dioxide was the suitable quantity for ensuring the best sensitivity of heterostructures. The sensor of the mentioned composition showed the highest sensitivity to carbon monoxide (min. 5 ppm).

The successful combination of dimensional effect of nanostructure and transit properties of n–n heterojunctions SnO_2-ZnO is used by authors [27] for creation gas-sensitive one-dimensional (1D) n–n SnO_2-ZnO heterostructures perspective for highly effective sensors of organic amine compounds. The heterostructures were ZnO nanowires (80–100 nm in diameter, 12–16 μm long) coated with layers of SnO_2 nanoparticles (about 4 nm) by effective solvothermal treatment followed by calcination at 400 °C. The size of tin dioxide nanoparticle, comparable with the Debye length in this material (~3 nm), provides almost complete particle depletion by electrons due to various surface adsorbed oxygen species $O^{\delta-}$(O_2^-, O^- and O^{2-}). Additional depletion is created at the SnO_2/ZnO heterointerface due to different work functions of ZnO (5.2 eV) and SnO_2 (4.9 eV). The energy band structures and gas sensing mechanisms of the SnO_2-ZnO NW heterostructure sensor is shown at Fig. 9.5.

A greater amount of oxygen can be adsorbed by the wire 1D structures both due to a lower agglomeration tendency and to a larger surface to volume ratio. All this facilitates the gas diffusion through a sensor and promotes active superficial reactions. The above mentioned features of one-dimensional (1D) n–n nanowire heterostructures of SnO_2-ZnO allowed to create on their basis a sensor of organic amine compounds with the improved characteristics: high speed of reaction and recovery, good selectivity and excellent reproducibility for n-butylamine vapors.

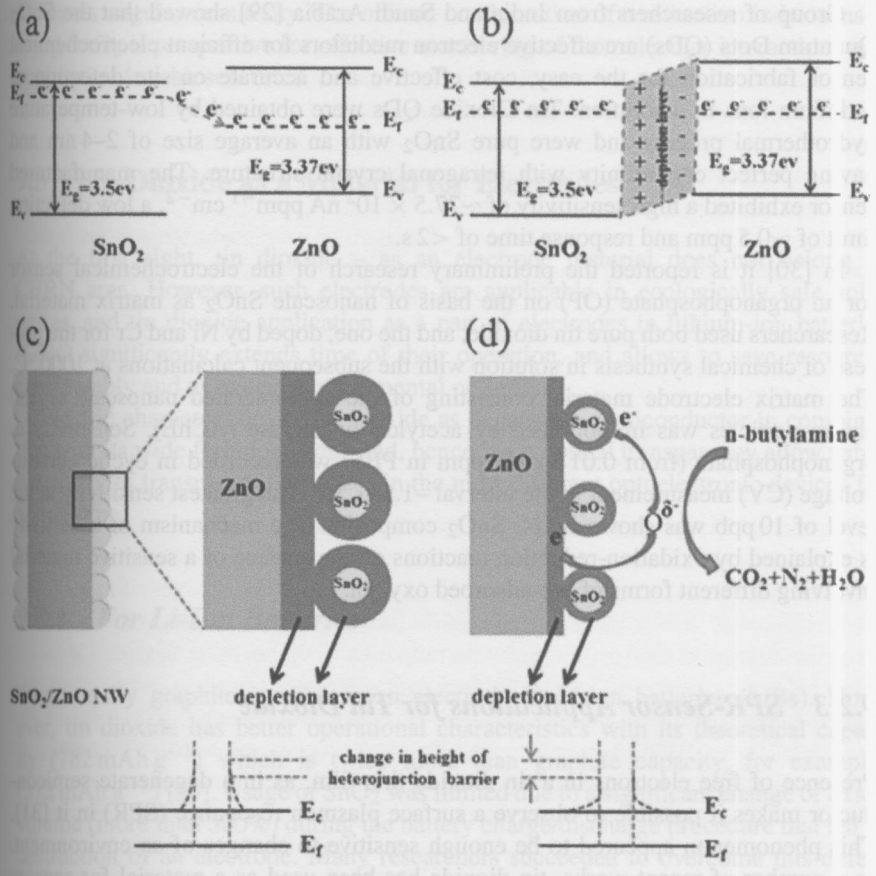

Fig. 9.5 (**a**, **b**) The energy band structures and (**c**, **d**) gas sensing mechanisms of the SnO_2-ZnO NW heterostructure sensor [27]

9.2.2 *Tin Dioxide as Electrochemical Sensors of Organic Compounds and Heavy Metals*

Enough often tin dioxides are used in electrochemical type sensors for heavy metals and dangerous organic compounds detection in various environments. Researchers from China [28] has conducted a complex of experimental and theoretical studies (adsorption/desorption tests, density-functional theory (DFT) calculations, and X-ray absorption of fine structure (XAFS) studies), thus revealing the electrochemical mechanism of heavy metals' ions interaction on various faces of tin dioxide nanocrystal. Researches showed that the face {110} has the lowest potential barrier for ions' superficial diffusion, hence showing the best electrochemical characteristics for detection of heavy metals ions.

Group of researchers from India and Saudi Arabia [29] showed that the SnO_2 Quantum Dots (QDs) are effective electron mediators for efficient electrochemical sensor fabrication for the easy, cost effective and accurate on-site detection of cadmium ions in a solution. Tin Dioxide QDs were obtained by low-temperature hydrothermal process and were pure SnO_2 with an average size of 2–4 nm and having perfect crystallinity with tetragonal crystal structure. The manufactured sensor exhibited a high sensitivity of $\sim 77.5 \times 10^2$ nA ppm^{-1} cm^{-2}, a low detection limit of ~0.5 ppm and response time of <2 s.

In [30] it is reported the preliminary research of the electrochemical sensor for an organophosphate (OP) on the basis of nanoscale SnO_2 as matrix material. Researchers used both pure tin dioxide, and the one, doped by Ni and Cr for the process of chemical synthesis in solution with the subsequent calcinations at 1000 °C. The matrix electrode material consisting of the agglomerated nanoscale crystal nature particles was immobilized by acetylcholinesterase (AChE). Sensitivity to organophosphate (from 0.01 to 100 ppm in PBS) was recorded in cyclic current-voltage (CV) measurement in the interval –1.5–1.5 V. The greatest sensitivity at the level of 10 ppb was shown by Ni-SnO_2 composite. The mechanism of sensitivity is explained by oxidation-reduction reactions on the surface of a sensitive material involving different forms of pre-adsorbed oxygen.

9.2.3 SPR-Sensor Applications for Tin Dioxide

Presence of free electrons in a tin dioxide thin-film, as in a degenerate semiconductor makes it possible to observe a surface plasmon resonance (SPR) in it [31]. This phenomenon appeared to be enough sensitive to changes of an environment. In a number of recent works, tin dioxide has been used as a material for sensors of biological media composition based on the SPR phenomenon [32, 33]. The measured sensitive value in such sensors is the refraction index of a material contacting with the controlled environment.

Using tin dioxide [33] as a sensing element in a fiber optic in SPR technique makes it possible to obtain a miniature probe for online monitoring, remote sensing of ammonia with high sensitivity, selectivity, stability, durability and low cost. Since the SPR characteristics depend significantly on the thickness of the sensitive material layer, then the probes with different thicknesses of SnO_2 have been investigated. Electromagnetic field distribution for the multilayer structure of the probe reveals the enhancement of evanescent field at the tin oxide-ammonia gas interface which in its turn manifests the highest shift in resonance wavelength at a definite thickness.

A theoretical analysis of a thin-film SnO_2 sensor for detection of volumetric media refraction index was presented in [34]. The analysis was carried out on the basis of Fresnel's equations for reflection coefficients. It showed that tin dioxide usage as the dielectric matching layer between a prism and the waveguide layer

increases angular sensitivity. The offered configuration of a refraction index sensor using SnO_2 is perspective for effective monitoring of biomolecular interactions and application in a biosensorics.

9.3 Tin Dioxide as a Material for Electrodes

At the first sight, tin dioxide – as an electrode material does not belong to CBRN area. However, such electrodes are applicable in ecologically safe solar power, and tin dioxide application as a part of electrodes in lithium-ion batteries (LiBs) significantly extends time of their operation, and allows to save resources considerably and to reduce environmental pollution.

Electric characteristics of tin dioxide as degenerate semiconductor in combination with its wide forbidden zone and, hence, with optical transparency allow using it actively as transparent electrodes in the most different optoelectronic devices for a long time.

9.3.1 For Li-Ion Batteries

Traditionally graphite is used as an electrode in Li-ion batteries (LiBs). However, tin dioxide has better operational characteristics with its theoretical capacity ($782\,mAh\,g^{-1}$) which is twice more than graphite capacity, for example, ($372\,mAh\,g^{-1}$) [35]. Usage of SnO_2 was limited due to a significant change of oxide volume (more than 300%) during the battery charge/discharge procedure that led to destruction of an electrode. Many researchers succeeded to overcome this defect using various nanoporous structures based on tin dioxide or with the embedded tin dioxide nanoparticles, also nanotubes, shell/core nanostructures, etc. [36–39]. In the majority of such structures the size of the embedded SnO_2 particles does not exceed 4–5 nm, since a larger size can not secure the reversibility of Sn/SnO_2 conversion process [40, 41]. The usage of tin dioxide in complex nanocomposites made it possible to increase the operational capacity of the electrodes to a level approaching 2000 mAh/g. In addition to high throughput, SnO_2-containing electrodes have another qualitive advantage for lithium-ion batteries – a long-term multiple cyclicity. As it was well summarized in [41], the nanostructured SnO_2 with a high reversibility of Sn/SnO_2, suppressed aggregation of Sn and stable passivating solid-electrolyte interphase (SEI) layer during cycling would be an ideal material for realization of high-performance LiBs.

After A. Geim and K. Novoselov reported in 2004 [42] on the production of graphene fixed on silicon oxide layers, such a material became widely used in electronics. In 2009 [35] it was reported on the creation of a composite material of graphene nanosheets and SnO_2 nanoparticles used as an anode material for LiBs. The Japanese researchers created nanoporous mobile 3-D structure as SnO_2 nanoparticles (3.3–7.5 nm) composite which are uniformly located between

graphene sheets. Nanopores between SnO_2 and nanosheets can play a role of buffer space in the charging/discharging process that significantly increases efficiency, capacitive properties and strength of such material (810 mAh/g) compared with usual SnO_2. In subsequent years several more groups of scientists used tin dioxide nanoparticles in graphene nanosheets for creation of highly effective electrodes for LiBs [36–38], at that, reversible capacities of the created electrodes exceed the theoretical capacity of SnO_2 almost by 1.5–2 times.

Enough complex three-dimensional graphene-like network structures with uniformly built-in SnO2@Sn nanoparticles doped by nitrogen, and encapsulated by carbon (N-C) were created and studied in work [39, 43] as anodes of high-performance LiBs. Structures, denoted as N-CSnO_2Sn/3D-GNs, has been fabricated by means of a low-cost and scalable method: an in situ hydrolysis of Sn salts and immobilization of SnO_2 nanoparticles on the surface of 3D-GNs, followed by an in situ polymerization of dopamine on the surface of the SnO_2/3D-GNs, and finalized by carbonization. The created composites promoted highly efficient insertion/extraction of Li(+). It is provided by three-layer structure of composite nanoparticles. The outermost N-C layer with graphene-like structure of the N-CSnO_2Sn nanoparticles can effectively buffer the large volume changes, enhance electronic conductivity, and prevent SnO_2/Sn aggregation and pulverization during discharge/charge. The middle layer function (namely tin dioxide) was to facilitate the cyclic charge/discharge process by participating in the reaction $SnO_2 + Li(+) \rightarrow Sn + Li_2O$. The inner Sn layer with large theoretical capacity can guarantee high lithium storage in the composite. This novel hybrid anode exhibits highly stable capacity of up to 901 mAh/g, with ~89.3% of capacity retention after 200 cycles at 0.1 A/g and superior high performance rate, as well as a long lifetime of 500 cycles with of 84.0% retention at 1.0 A/g. Such high operational rates are combined with structural integrity of the whole electrode in which tin dioxide plays an important role.

However, electrodes with good performance may be obtained not only of a graphene. Asymmetric membrane structure for stabilization of the LiBs anode based on SnO_2 with excellent electrochemical characteristics was created in [40] using a combined sol-gel technique followed by carbonization. The reached specific capacity of an asymmetric membrane electrode on tin dioxide in 500 mAh/g managed to be kept at the level of 96% after 400 cycles at a current density of 280 mA/g (~0.5 C). The current density doubling leads to a decrease in the general power only by 36%. The membrane has mesh porous structure which provides high conductivity, multiple channels for diffusion and free volumes for an electrode expansion. The main technological step influencing properties of an electrode is the carbonization temperature. The membrane electrode shows the best characteristics in case of carbonization at 500 °C. At the same time the size of SnO_2 nanoparticles is ~3.9 nm. At temperature increase to 800 °C electrode loses 51% of the capacity for 100 cycles due transformation of nanoparticles into large tin spheres (~40 nm).

In February 2017 Wei and colleagues [44] reported the inexpensive way of synthesizing of uniform anode material for LiBs from ultrasmall (~3 nm) particles of SnO_2 which are uniformly distributed in polymer of a styrylpyridinium (SbQ).

Formation of an electrode was carried out by UF hardening method. Ability of SbQ polymer to a photocrosslinking in-situ allowed synthesizing uniform ultramassive material. Styrylpyridinium being strong binding for SnO_2 nanoparticles provides effective change of SnO_2 anodes' volume during cyclic charge- discharge process. Steady specific capacity 572.5 mAh/g of the created SnO_2 electrode is obtained at the current density of 0.2 C (156.2 mA/g) after 150 cycles. Even at high current density 5 C (3905 mA/g) the specific capacity is 440.2 mAh/g.

The priority requirements to anode materials of LiBs were realized by the Korean researchers [45] having synthesized anodes on SnO_2/NiO nanotube (m-SNT decorated by mesoporous Ag nanoparticles). The material was synthesized by an electrospinning treatment followed by fast calcination and subsequent chemical reduction. Such a problem as considerable change of volume at cycling is effectively reduced in one-dimensional porous hollow structure. This structure also provides a short lithium-ion diffusion length. The reversible capacity of the m-SNT anodes was significantly improved using metallic nickel (Ni) nanoparticles converted from NiO nanograins during the lithiation process of Li_2O reversible decomposition. Ag nanoparticles uniformly decorated on the m-SNT via a simple chemical reduction process significantly improve rate capability and also contribute to long-term cyclability. The m-SNTAg anodes exhibited excellent cycling stability without capacity fading after 500 cycles with a high capacity of 826 mAh/g at a high current density of 1000 mA/g. Furthermore, even at a very high current density of 5000 mA/g, charge-specific capacity remained as high as 721 mAh/g, corresponding to 60% of its initial capacity at a current density of 100 mA/g. The Fig. 9.6 shows schematic illustration for the synthetic route of the m-SNT@Ag and long-term cycling stability of the m-SNTAg at a current density of 500 mA/g [45].

Thus, the nanostructured SnO_2 with high reversibility of Sn/SnO_2 obtained due to the suppressed aggregation of Sn and to stable layer of SEI at cycling would be an ideal material for high-performance LiBs.

Problems of tin-dioxide's volume change in electrodes of LiBs, and at the same time the satisfaction of the requirement to their charging efficiency and cyclic stability were solved in [41] by creation of polydophamine (PDA) – coated SnO_2

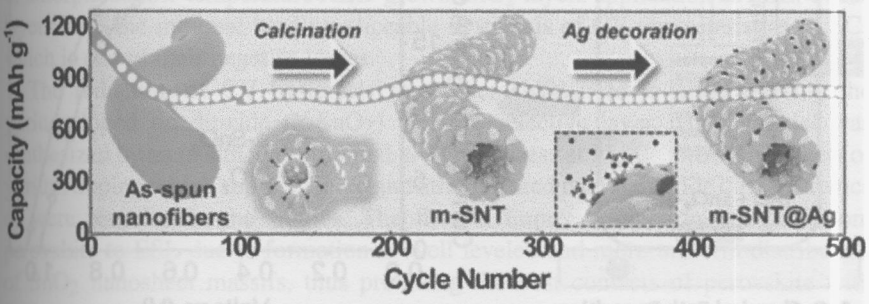

Fig. 9.6 Schematic illustration for the synthetic route of the m-SNTAg and long-term cycling stability of the m-SNTAg at a current density of 500 mA/g [45]

nanocrystals, composed of hundreds of PDA-coated "corn-like" SnO_2 nanoparticles (diameter ~5 nm) decorated along a "cob". In a combination, the corn-like nanostructure and PDA protection provided excellent electrochemical characteristics of SnO_2 electrode together with excellent long-term cyclic stability throughout more than 300 cycles, high reversibility of Sn/SnO_2 and excellent speed.

9.3.2 *For Solar Cells*

Unique combination of electrophysical properties of tin dioxide as degenerate semiconductor (small work function, high density of electrons in the forbidden zone) and considerable optical width of its forbidden zone (~4 eV), a possibility of obtaining thin layer coatings makes this material to be very convenient as electron transporting layer (ETL) for solar elements, especially new perovskits solar elements – perspective cheap silicon substitutes [46–48]. Many researchers note positive impact of low-temperature technologies of SnO_2 nanolayers production for electron selective layers [46–51].

Thin films of amorphous tin dioxide were offered in [47] as electron transporting layer (ETL) in planar heterojunction n-i-p organohalide lead perovskite and organic bulk heterojunction solar cells. Films were prepared by chemical bath deposition from a non-toxic aqueous bath of tin chloride at very low temperatures (55 °C) and do not require post-annealing treatment. Low mobility of electrons, specific for SnO_2 film samples, is successfully compensated by low work function with ideal alignment of zones on the border of SnO_2/methylammonium lead iodide ($MAPbI_3$) and strong blocking of holes due to the deep SnO_2 valence zone. The schematic picture of an amorphous SnO_2 film deposition method and the volt-current characteristics of a solar cell with a-SnO_2 ETL are given at the Fig. 9.7 from

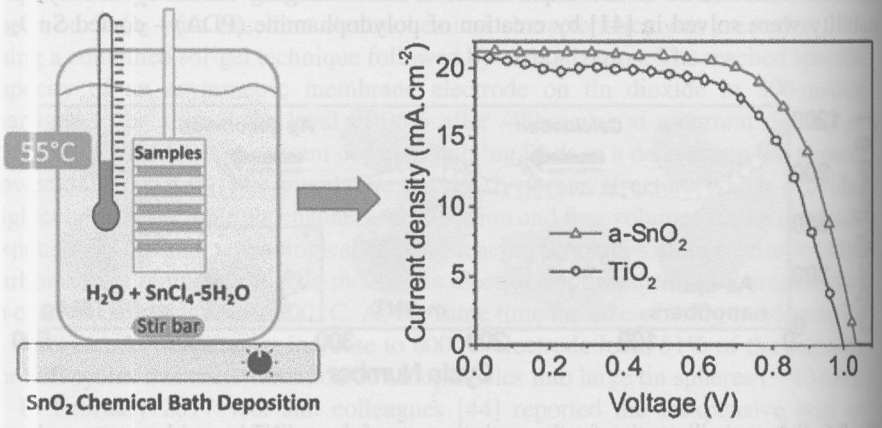

Fig. 9.7 The schematic picture of SnO_2 amorphous film deposition method and the volt-current characteristic of a solar cell with a-SnO_2 ETL [47]

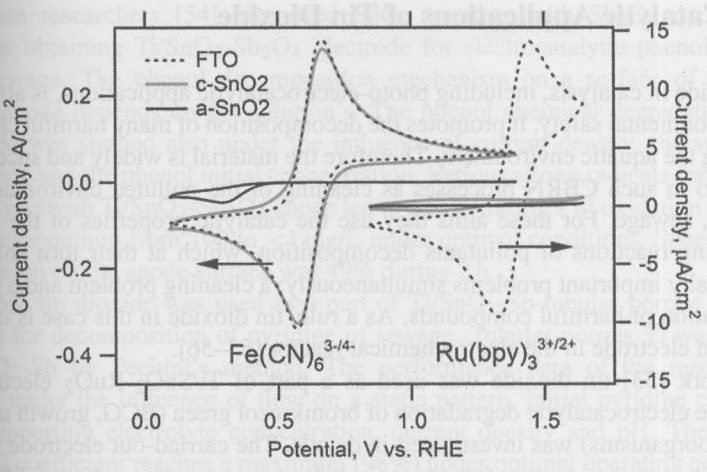

Fig. 9.8 CV characteristics of SCs with different electron selective layers [52]

[47]. It is seen that usage of a-SnO_2 ETL prepared by chemical bath deposition provides a solar cell with the better operational characteristics in comparison with TiO_2 ETL.

Group of the Swiss and Czech scientists led by M. Grätzel (the famous creator of the same name electrochemical solar cell) [52] presented in 2017 an ultrathin electron selective layers (ESL) of SnO_2 fabricated by atomic layer deposition (ALD) for application in planar perovskite solar cells as powerful alternatives to other oxides such as TiO_2. The obtained layers besides being used for photoelectrodes in perovskite and dye-sensitized solar cells also may be applied in photoelectrochemical water splitting. The various studies of the layers' physical properties showed that not calcinated low-temperature ALD-grown SnO_2 layers are amorphous and perfectly pinhole-free for thicknesses down to 2 nm. Such a thickness and electric properties of layers allows designing a photoelectrode with thinner electron selective layers that potentially minimizes resistance losses. Figure 9.8 shows the advantages of amorphous low-temperature ALD-grown SnO_2 layers application as ESL. These layers have the minimal hardly noticeable hysteresis of CV characteristics of SCs which is one of their negative issues.

The reduction of CV hysteresis researchers [49] tried to achieve using the yttrium-doped tin dioxide (Y-SnO_2) electron selective layer. This material was synthesized by an in situ hydrothermal growth process at 95 °C. Two main effects of yttrium doping which supplemented and strengthened the tin dioxide characteristics of were revealed in the studies. The first, it improves electrons transfer from perovskite to ESL due to formation of well leveled and more uniform distribution of SnO_2 nanosheet massifs, thus providing the best contacts of perovskite with SnO_2 nanosheet, secondly, it secures the charges recombination decrease at NSA-perovskite interfaces due to the forbidden zone growth and to the switching of the band energy levels up, and their alignment by perovskite energy levels.

9.4 Catalytic Applications of Tin Dioxide

Tin dioxide in catalysis, including photo-electrocatalytic applications, is also useful for environmental safety. It promotes the decomposition of many harmful chemicals polluting the aquatic environment. Therefore the material is widely and successfully used also in such CBRN processes as cleaning of the polluted environments, for example, sewage. For these aims they use the catalytic properties of the material stimulating reactions of pollutants decomposition, which at their turn solves two ecologically important problems simultaneously: a cleaning problem and a problem of utilization of harmful compounds. As a rule, tin dioxide in this case is used as a part of an electrode in the electrochemical reactor [53–56].

In work [53] tin dioxide was used as a part of Ti/SnO_2-RuO_2 electrode for which the electrocatalytic degradation of bromkrezol green (BCG, growth mediums for microorganisms) was investigated in details. The carried-out electrode material characterization by means of the scanning electron microscopy, X-ray diffractometry and X-ray fluorescence spectrometry showed "cracking dirt" structure and excellent specific surface area of Ti/SnO_2-RuO_2 electrode. Efficiency of BCG removal from the Ti/SnO_2-RuO_2 electrode was determined basing on chemical consumption of oxygen and on ultra-violet-visible absorbing spectrometry (UV-Vis spectroscopy changes are shown in the Fig. 9.9).

The major factors defining the BCG removal efficiency were in descending order: initial pH_0, reaction temperature, and current density and electrolysis duration time. The BCG removal efficiency reached 91% under optimal experimental conditions (initial concentration – 100 mg/L, initial pH_0 – 7, temperature of reaction – 30 °C, current density – 12 m/cm^2 and the electrolysis time – 150 min).

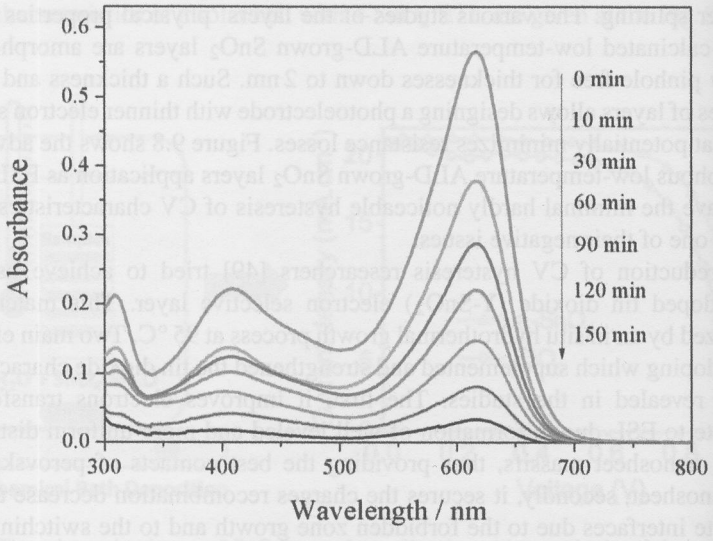

Fig. 9.9 UV-Vis spectroscopy changes of BCG electrocatalytic degradation [53] with electrolysis time

Iranian researchers [54] also used SnO_2 together with Sb_2O_4 on a titanic plate for obtaining Ti/SnO_2-Sb_2O_4 electrode for electrocatalytic phenol removal from sewage. The phenol decomposition mechanism on a surface of Ti/SnO_2-Sb_2O_4 anode depends on the solution's. The phenol chemical degradation on an electrode was studied also under the influence of current density, the supporting electrolyte and the phenol initial concentration. Various strong radicals formation in electrolysis with Ti/SnO_2-Sb_2O_4 anode led to quick (during 1 h) oxidation of phenol up to benzoquinon from 100 to <1 mg/L under optimal conditions. Speed of TOS degradation on the anode surface was 49% during 2 h.

In [55] tin dioxide was used as a part of Ti/SnO_2-Sb tubular porous electrode (anode) for decomposition of pyridine of sewage. Tubular porous Ti was covered by SnO_2-Sb by Pechini's method. The performance data of the reactor were studied under the influence of flow on a static pattern, initial pyridine concentration, supporting electrolyte concentration, current density and pH. The pyridine removal coefficient reaches a maximum (98%) under optimal operating conditions: 100 mg/L of pyridine initial concentration, 10 g/L, the supporting concentration of electrolyte, 30 m/cm^2 density of current and pH 3.

Chinese researchers [56] applied tin dioxide for creation of the nanostructured high-porous 3D electrode of the Ti/Sb-SnO_2-GR based on three-dimensional porous graphene hydrogel. The electrode was formed by layer-by-layer sedimentation. The 3D porous electrode has the high potential for oxygen release (2.40 V), smaller resistance to charge transfer (29.40 Ohms·cm^2), higher porosity (0.90), the elevated coefficient of a roughness (181) and higher charge value (57.4 mC/cm^2) in comparison with flat Ti/Sb-SnO_2 electrode. Electrocatalytic oxidation of rhodamine B (RhB) as a test electrochemical reaction also showed better characteristics, stability and low specific power consumption.

The SnO_2 nanoparticles microspheres decorated by Ag, obtained by a simple hydrothermal (one-pot hydrothermal method) [57] were successfully applied in catalytic reduction of 4-nitrophenol to 4-aminophenol by potassium borohydride (KBH_4) as a model reaction. The known toxic pollutant 4 nitrophenol (4-NP), is widely present in industrial drains and agricultural sewage, and its chemical reduction to 4-aminophenol (used for production of analgetics, cosmetic and anticorrosive materials) is the most preferable. The catalytic characteristics of the obtained composite structures were enough high, so that normalized rate constant (κ_{nor}) was 6.20 L/(min g). Besides the mentioned, they demonstrate good renewability after the first five cycles.

Tin dioxide usage in various structures improves the production characteristics of gaseous hydrogen [58] and ozone [59] which is useful both as for power, and ecological safety.

In [58] tin dioxide was applied as a part of one-dimensional nanowires with core-cover type structure of the CeO_2/SnO_2 grown up on a three-dimensional porous disk in the form of the nano-wood. The structure was effectively used for obtaining H_2 by thermochemical separation of water at temperatures up to 800 °C. Three-dimensional a core- cover type "nanowire wood" increased the production of H_2 by 45.5% at 800 °C in comparison with usual thin-film CeO_2 covered disks as standards.

Theoretical calculations using a theory of the density functional were applied by Gibson and colleagues [59] to analyze electrochemical mechanism of ozone production by decomposition of water on the SnO_2 catalyst doped by Ni and Sb. The SnO_2 face (110) appeared to be the most stable according to calculations. This surface was used for water decomposition modeling in the presence of doping by Sb and Ni, paying special attention to stages of O_2 and O_3 formation. The ozone formation takes place according to the Langmuir–Hinshelwood's mechanism, i.e. on the surface of the catalyst. The adsorption energy calculation (EADS), the Gibbs' free energy (ΔG_{rxn}) and barriers of activation (E_{act}) obtained for two final stages of ozone formation serves as a basis for new materials development with higher catalytic efficiency.

9.5 The Nanostructured Thin Films of Tin Dioxide

Authors have conducted a series of studies of tin dioxide thin films obtained using polyvinil acetate (PVA) polymers in sol-gel method to improve structuring.

In the said studies the content of the precursor (Bisacetylacetonato dichlorotin (BADCT)) in the initial solution varied from 1 to 10%. The polymer (PVA) content in the solution was 1%. After deposition on the glass substrate, the samples were annealed until the organic components were removed and a transparent tin dioxide layer was formed. AFM three dimensional tin dioxide film's surface picture is shown at Fig. 9.10.

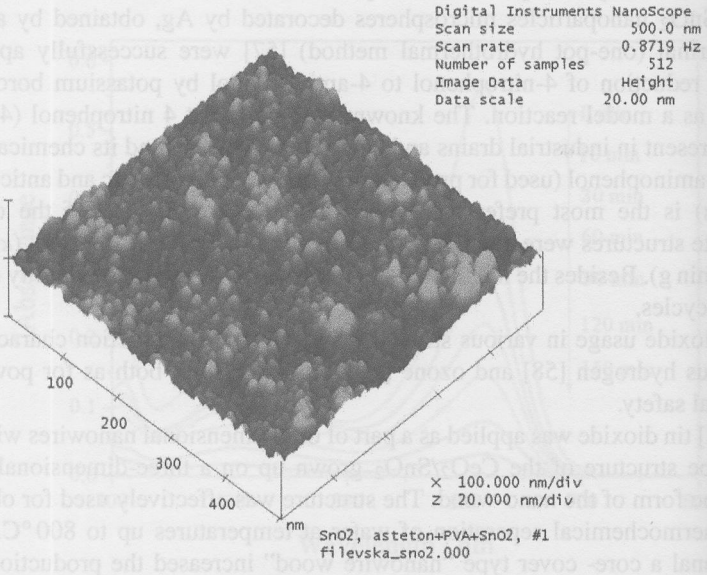

Fig. 9.10 AFM three dimensional tin dioxide film's surface picture

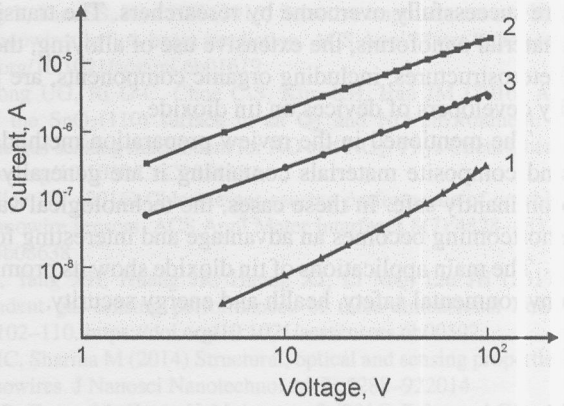

Fig. 9.11 CV characteristic of the SnO_2 film ($T = 290$ K): *1* – in the air, *2* – after heating to 410 K at the pressure of about 10^{-3} mm Hg and again, cooling to room temperature, *3* – in 15 min after the atmospheric air was let into the chamber [60]

Preliminary researches showed that these films may be essentially applicable as CBRN material, in a gas sensorics, at least.

The conductivity of the studied films in vacuum and in the air differs by more than an order of magnitude, which indicates the considerable influence of adsorption interaction with oxygen in the air [60]. Figure 9.11 shows CV characteristics of the SnO_2 film at room temperature.

The films' conductivity changes during heating and subsequent cooling at vacuum up to the initial temperature are reversible and repeatable, which shows the electrical characteristics of the SnO_2 films stability and allows using them as adsorptive-sensitive elements for gas sensors.

The obtained films of the nanostructured tin dioxide demonstrate the photoluminescence (~1.9 and ~2.2) eV at a room temperature. This makes them perspective as for their application as PhL sensors for non contact mediums content control.

The SPR parameters were studied on the films by means of polarization- modular spectroscopy (PMS) in the work [61]. The SPR phenomena established in the films of tin dioxide makes it possible to use them as a sensor material in SPR transducers of gases and biological mediums.

9.6 Conclusion

The results of papers for the latest two years show the effectiveness of tin dioxide usage to ensure safety as a convenient, cheap, common material with suitable physicochemical properties. The use of nanoscale forms of SnO_2 as a material for gas sensors of conductometric type, electrochemical sensors, sensors on the SPR effect, the material for electrodes of lithium-ion batteries and solar cells, catalysts for the pollutant decomposition is considered.

Dependence of its properties on manufacturing technology, significant volume change when used in LiBs electrodes, low selectivity to different hydrocarbons,

are successfully overcome by researchers. The transition to the creation of various material nanoforms, the extensive use of alloying, the formation of composites and heterostructures, including organic components, are just some of the methods used by developers of devices on tin dioxide.

The mentioned in the review preparation methods of nanoscale forms of SnO_2 and composite materials containing it are generally simple, inexpensive and predominantly safe. In these cases, the technological variability of tin dioxide from a shortcoming becomes an advantage and interesting for further study.

The main applications of tin dioxide show its promising as a material for ensuring environmental safety, health and energy security.

References

1. Jarzebski ZM, Marton JP (1976) Physical properties of SnO_2 materials. I. Preparation and defect structure. J Electrochem Soc 123(7):199–205. https://doi.org/10.1149/1.2133010
2. Comini E (2006) Metal oxide nano-crystals for gas sensing. Anal Chim Acta 568:28–40
3. Hwang I-S, Lee J-H (2011) Gas sensors using oxide nanowire networks: an overview. J Nanoeng Nanomanuf 1:4–17. https://doi.org/10.1166/jnan.2011.1002
4. Sun Y-F, Liu S-B, Meng F-L, Liu J-Y, Jin Z, Kong L-T, Liu J-H (2012) Metal oxide nanostructures and their gas sensing properties: a review. Sensors 12:2610–2631. https://doi.org/10.3390/s120302610
5. Woo HS, Na CW, JH Lee (2016) Design of highly selective gas sensors via physicochemical modification of oxide nanowires: overview. Sensors 16:1531–23. https://doi.org/10.3390/s16091531, www.mdpi.com/journal/sensors.
6. Granqvist CG (2007) Transparent conductors as solar energy materials: a panoramic review. Sol Energy Mat Sol Cells 91:1529–1598.
7. Ginley D, Hosono H, Paine DC (eds) (2011) Handbook of transparent conductors. Springer, New York
8. Papargyri S, Tsipas DN, Papargyris DA, Botis AI, Papargyris AD (2005) Review on the production and synthesis of nanosized SnO_2. Solid State Phenom 106:57–62
9. Batzill M, Diebold U (2005) Review: the surface and materials science of tin oxide. Prog Surf Sci 79:47–154
10. Pan J, Shen H, Mathur S (2012) One-dimensional SnO_2 nanostructures: synthesis and applications. J Nanotechnol 2012. Article ID 917320. https://doi.org/10.1155/2012/917320, www.hindawi.com/journals/jnt/2012/917320/
11. Das S, Jayaraman V (2014) SnO_2: a comprehensive review on structures and gas sensors. Prog Mat Sci 66:112–255. https://doi.org/10.1016/j.pmatsci.2014.06.003
12. Nazarov DV, Bobrysheva NP, Osmolovskaya OM, Osmolovsky MG, Smirnov VM (2015) Atomic layer deposition of tin dioxide nanofilms: a review. Rev Adv Mater Sci 40:262–275
13. Mohanta D, Ahmaruzzaman M (2016) Tin oxide nanostructured materials: an overview of recent developments in synthesis, modifications and potential applications. RSC Adv 6:110996–111015. https://doi.org/10.1039/C6RA21444D
14. Dastkhoon M, Ghaedi M, Asfaram A, Arabi M, Ostovan A, Goudarzi A (2017) CuSnS/SnO_2 nanoparticles as novel sorbent for dispersive micro solid phase extraction of atorvastatin in human plasma and urine samples by high-performance liquid chromatography with UV detection: application of central composite design (CCD). Ultrason Sonochem 36:42–49. https://doi.org/10.1016/j.ultsonch.2016.10.030

15. Kwon YJ, Kang SY, Wu P, Peng Y, Kim SS, Kim HW (2016) Selective improvement of NO_2 gas sensing behavior in SnO_2 nanowires by ion-beam irradiation. ACS Appl Mater Interfaces 8(21):13646–13658. https://doi.org/10.1021/acsami.6b01619
16. Hong SN, Kye YH, Yu C-J, Jong UG, Ri G-C, Choe C-S, Kim KH, Han JM (2016) Ab initio thermodynamic study of the SnO_2(110) surface in an O_2 and NO environment: a fundamental understanding of the gas sensing mechanism for NO and NO_2. Phys Chem Chem Phys 18:31566–31578. https://doi.org/10.1039/C6CP05433A
17. Dang TV, Hoa ND, Duy NV, Hieu NV (2016) Chlorine gas sensing performance of on-chip grown ZnO, WO_3, and SnO_2 nanowire sensors. ACS Appl Mater Interfaces 8(7):4828–4837. https://doi.org/10.1021/acsami.5b08638
18. Li YX, Guo Z, Su Y, Jin XB, Tang XH, Huang JR, Huang XJ, Li MQ, Liu JH (2017) Hierarchical morphology-dependent gas-sensing performances of three-dimensional SnO_2 nanostructures. ACS Sens 2(1):102–110. https://doi.org/10.1021/acssensors.6b00597
19. Johari A, Johari A, Bhatnagar MC, Sharma M (2014) Structural, optical and sensing properties of pure and Cu-doped SnO_2 nanowires. J Nanosci Nanotechnol 14(7):5288–922014
20. Bhardwaj N, Pandey A, Satpati B, Tomar M, Gupta V, Mohapatra S (2016) Enhanced CO gas sensing properties of Cu doped SnO_2 nanostructures prepared by a facile wet chemical method. Phys Chem Chem Phys 18(28):18846–54. https://doi.org/10.1039/c6cp01758d
21. Yang F, Guo Z (2015) Comparison of the enhanced gas sensing properties of tin dioxide samples doped with different catalytic transition elements. J Colloid Interface Sci 448:265–74. https://doi.org/10.1016/j.jcis.2015.02.045
22. Degler D, Rank S, Müller S, de Carvalho HWP, Grunwaldt JD, Weimar U, Barsan N (2016) Gold-loaded tin dioxide gas sensing materials: mechanistic insights and the role of gold dispersion. ACS Sens 1(11):1322–1329. https://doi.org/10.1021/acssensors.6b00477
23. Teterycz H, Licznerski BW (2006) Properties of selective gas-sensitive SnO_2/RuO_2/Pt composition and detection mechanism. J Electrochem Soc 153(5):H94–H104
24. Lyson-Sypien B, Kusior A, Rekas M, Zukrowski J, Gajewska M, Michalow-Mauke K, Graule T, Radecka M, Zakrzewska K (2017) Nanocrystalline TiO_2/SnO_2 heterostructures for gas sensing. Beilstein J Nanotechnol 8:108–122. https://doi.org/10.3762/bjnano.8.12
25. Chen W, Li Q, Xu L, Zeng W (2015) Gas sensing properties of ZnO-SnO_2 nanostructures. J Nanosci Nanotechnol 15(2):1245–1252
26. Chesler P, Hornoiu C, Mihaiu S, Vladut C, Calderon Moreno JM, Anastasescu M, Moldovan C, Firtat B, Brasoveanu C, Muscalu G, Stan I, Gartner M (2016) Nanostructured SnO_2-ZnO composite gas sensors for selective detection of carbon monoxide. Beilstein J Nanotechnol 7:2045–2056. https://doi.org/10.3762/bjnano.7.195
27. Wang L, Li J, Wang Y, Yu K, Tang X, Zhang Y, Wang S, Wei C (2016) Construction of 1D SnO_2-coated ZnO nanowire heterojunction for their improved n-butylamine sensing performances. Sci Rep 6:35079. https://doi.org/10.1038/srep35079
28. Jin Z, Yang M, Chen SH, Liu JH, Li QX, Huang XJ (2017) Tin oxide crystals exposed by low-energy {110} facets for enhanced electrochemical heavy metal ions sensing: X-ray absorption fine structure experimental combined with density-functional theory evidence. Anal Chem 89(4):2613–2621. https://doi.org/10.1021/acs.analchem.6b04977
29. Bhanjana G, Dilbaghi N, Kumar R, Umar A, Kumar S (2015) SnO_2 quantum dots as novel platform for electrochemical sensing of cadmium. Electrochim Acta 169:97–102. https://doi.org/10.1016/j.electacta.2015.04.045
30. Khan N, Athar T, Fouad H, Umar A, Ansari ZA, Ansari SG (2017) Application of pristine and doped SnO_2 nanoparticles as a matrix for agro-hazardous material (organophosphate) detection. Sci Rep 7:42510. https://doi.org/10.1038/srep42510
31. Grinevich VS, Filevska LM, Matyash IE, Maximenko LS, Mischuk ON, Rudenko SP, Serdega BK, Smyntyna VA, Ulug B (2012) Surface plasmon resonance investigation procedure as a structure sensitive method for SnO_2 nanofilms. Thin Solid Films 522:452–456
32. Yang D, Lu H-H, Chen B, Lin C-W (2010) Surface plasmon resonance of SnO_2/Au bi-layer films for gas sensing applications. Sensors and Actuators B Chem 145(2):832–838

33. Pathak A, Mishra SK, Gupta BD (2015) Fiber-optic ammonia sensor using Ag/SnO_2 thin films: optimization of thickness of SnO_2 film using electric field distribution and reaction factor. Appl Opt 54(29):8712–8721. https://doi.org/10.1364/AO.54.008712
34. Kaur D, Madaan D, Sharma VK, Kapoor A (2016) High angular sensitivity thin film tin oxide sensor. In: Proceeding of international conference on condensed matter and applied physics (ICC 2015). AIP conference proceedings, vol 1728, p 020210. http://dx.doi.org/10.1063/1.4946261
35. Paek SM, Yoo EJ, Honma I (2009) Enhanced cyclic performance and lithium storage capacity of SnO_2/graphene nanoporous electrodes with three-dimensionally delaminated flexible, structure. Nano Lett 9(1):72–75. https://doi.org/10.1021/nl802484w
36. Lin J, Peng Z, Xiang C, Ruan G, Yan Z, Natelson D, Tour JM (2013) Graphene nanoribbon and nanostructured SnO_2 composite anodes for lithium ion batteries. ACS Nano 7(7):6001–6006. https://doi.org/10.1021/nn4016899
37. Xia G, Li N, Li D, Liu R, Wang C, Li Q, Lü X, Spendelow JS, Wu J, Zhang G (2013) Graphene/Fe_2O_3/SnO_2 ternary nanocomposites as a high-performance anode for lithium ion batteries. ACS Appl Mater Interfaces 5(17):8607–8614. https://doi.org/10.1021/am402124r
38. Zhou D, Song WL, Li X, Fan LZ Confined porous graphene/SnO_x frameworks within polyaniline-derived carbon as highly stable lithium-ion battery anodes. ACS Appl Mater Interfaces 8(21):13410–72016. https://doi.org/10.1021/acsami.6b01875
39. Li Y, Zhang H, Chen Y, Shi Z, Cao X, Guo Z, Shen PK (2016) Nitrogen-doped carbon-encapsulated SnO^2Sn nanoparticles uniformly grafted on three-dimensional graphene-like networks as anode for high-performance lithium-ion batteries. ACS Appl Mater Interfaces 8(1):197–207. https://doi.org/10.1021/acsami.5b08340
40. Wu J, Chen H, Byrd I, Lovelace S, Jin C (2016) Fabrication of SnO_2 asymmetric membranes for high performance lithium battery anode. ACS Appl. Mater. Interfaces 8(22):13946–13956. https://doi.org/10.1021/acsami.6b03310
41. Jiang B, He Y, Li B, Zhao S, Wang S, He Y, Lin Z (2017) Polymer-templated formation of polydopamine-coated SnO_2 nanocrystals: anodes for cyclable lithium-ion batteries. Angew Chem Int Ed Engl 56(7):1869–1872. https://doi.org/10.1002/anie.201611160
42. Novoselov KS, Geim AK, Morozov SV, Jiang D, Zhang Y, Dubonos SV, Grigorieva IV, Firsov AA (2004) Electric field effect in atomically thin carbon films. Science 306:666–669. https://doi.org/10.1126/science.1102896
43. Repetsky SP, Vyshyvana IG, Kruchinin SP, Molodkin VB, Lizunov VV (2017) Influence of the adsorbed atoms of potassium on an energy spectrum of grapheme. Metallofiz Noveishie Tekhnol 39:1017–1022
44. Wei H, Xia Z, Xia D (2017) One step synthesis of uniform SnO_2 electrode by UV curing technology toward enhanced lithium-ion storage. ACS Appl Mater Interfaces 9(8):7169–7176. https://doi.org/10.1021/acsami.6b15820
45. Kim C, Jung JW, Yoon KR, Youn DY, Park S, Kim ID (2016) A high-capacity and long-cycle-life lithium-ion battery anode architecture: silver nanoparticle-decorated SnO_2/NiO nanotubes. ACS Nano 10(12):11317–11326. https://doi.org/10.1021/acsnano.6b06512
46. Singh T, Singh J, Miyasaka T (2016) Role of metal oxide electron-transport layer modification on the stability of high performing perovskite solar cells. Chem Sus Chem 9(18):2559–2566. https://doi.org/10.1002/cssc.201601004
47. Barbe J, Tietze ML, Neophytou M, Murali B, Alarousu E, Labban A, Abulikemu M, Yue W, Mohammed OF, McCulloch I, Amassian A, Del Gobbo S (2017) Amorphous tin oxide as low temperature-processed electron transport layer for organic and hybrid perovskite solar cell. ACS Appl Mater Interfaces 9(13):11828–11836. https://doi.org/10.1021/acsami.6b13675
48. Lee Y, Paek S, Cho KT, Oveisi E, Gao P, Lee S, Park J-S, Zhang Y, Humphry-Baker R, Asiri AM, Nazeeruddin MK (2017) Enhanced charge collection with passivation of the tin oxide layer in planar perovskite solar cells. J Mater Chem A 5(25):12729–12734

49. Yang G, Lei H, Tao H, Zheng X, Ma J, Liu Q, Ke W, Chen Z, Xiong L, Qin P, Chen Z, Qin M, Lu X, Yan Y, Fang G (2017) Reducing hysteresis and enhancing performance of perovskite solar cells using low-temperature processed Y-doped SnO_2 nanosheets as electron selective layers. Small 13(2):1601769–1601769. https://doi.org/10.1002/smll.201601769
50. Rodionov VE, Shnidko IN, Zolotovsky A, Kruchinin SP (2013) Electroluminescence of Y_2O_3:Eu and Y_2O_3:Sm films. Mater Sci 31:232–239
51. Ermakov V, Kruchinin S, Fujiwara A (2008) Electronic nanosensors based on nanotransistor with bistability behaviour. In: Bonca J, Kruchinin S (eds) Proceedings of NATO ARW "Electron transport in nanosystems". Springer, pp 341–349
52. Kavan L, Steier L, Grätzel M (2017) Ultrathin buffer layers of SnO_2 by atomic layer deposition: perfect blocking function and thermal stability. J Phys Chem C 121(1):342–350. https://doi.org/10.1021/acs.jpcc.6b09965
53. Bai H, He P, Chen J, Liu K, Lei H, Zhang X, Dong F, Li H (2017) Electrocatalytic degradation of bromocresol green wastewater on Ti/SnO_2-RuO_2 electrode. Water Sci Technol 75(1):220–227. https://doi.org/10.2166/wst.2016.509
54. Loloi M, Rezaee A, Aliofkhazraei M, Rouhaghdam AS (2016) Electrocatalytic oxidation of phenol from wastewater using Ti/SnO_2-Sb_2O_4 electrode: chemical reaction pathway study. Environ Sci Pollut Res Int 23(19):19735–43. https://doi.org/10.1007/s11356-016-7110-6
55. Li D, Tang J, Zhou X, Li J, Sun X, Shen J, Wang L, Han W (2016) Electrochemical degradation of pyridine by Ti/SnO_2-Sb tubular porous electrode. Chemosphere 149:49–56. https://doi.org/10.1016/j.chemosphere.2016.01.078
56. Asim S, Zhu Y, Rana M, Yin J, Shah MW, Li Y, Wang C (2017) Nanostructured 3D-porous graphene hydrogel based Ti/Sb-SnO_2-Gr electrode with enhanced electrocatalytic activity. Chemosphere 169:651–659. https://doi.org/10.1016/j.chemosphere.2016.11.119
57. Hu M, Zhang Z, Luo C, Qiao X (2017) One-pot green synthesis of Ag-decorated SnO_2 microsphere: an efficient and reusable catalyst for reduction of 4-nitrophenol. Nanoscale Res Lett 12:435. https://doi.org/10.1186/s11671-017-2204-8
58. Seo K, Lim T, Mills EM, Kim S, Ju S (2016) Hydrogen generation enhanced by nano-forest structures. RSC Adv 6:12953–12958. https://doi.org/10.1039/C5RA26226G
59. Gibson G, Wang Z, Hardacre C, Lin WF (2017) Insights into the mechanism of electrochemical ozone production via water splitting on the Ni and Sb doped SnO_2 catalyst. Phys Chem Chem Phys 19(5):3800–3806. https://doi.org/10.1039/c6cp06906a
60. Filevska LM, Chebanenko AP, Grinevych VS, Simanovych NS (2016) The electrical characteristics of nanoscale SnO_2 films, structured by polymers. Photoelectronics 25:62–67
61. Grinevich VS, Filevska LM, Rudenko SP, Stetsenko MA, Maximenko LS, Serdega BK, Smyntyna VA (2016) Radiation modes of surface plasmons in SnO_2 thin films (in Ukrainian). In: 7th international scientific and technical conference on "Sensor Electronics and Microsystem Technologies" (SEMST-7), Book of Abstract, 30 May–3 June 2016, Odessa (Astroprint Odessa), p 181